

# STATIC BENDING ANALYSIS OF NANOPlates ON DISCONTINUOUS ELASTIC FOUNDATION WITH FLEXOELECTRIC EFFECT

**Van Minh Phung<sup>1,\*</sup>, Minh Thai Le<sup>2</sup>, Trac Luat Doan<sup>1</sup>, Dinh Anh Vu Nguyen<sup>3</sup>**

<sup>1</sup>*Faculty of Mechanical Engineering, Le Quy Don Technical University, Hanoi, Vietnam;*

<sup>2</sup>*Faculty of Special Equipment, Le Quy Don Technical University, Hanoi, Vietnam;*

<sup>3</sup>*Faculty of Weapons, Military Technical Officer School*

## **Abstract**

In this study, rectangular plates subjected to static loads and supported on a discontinuous two-parameter elastic foundation are analyzed. The formulae for the computations are developed from improved shear deformation theory, where the displacement  $w$  is divided into bending and shear strain components. The results obtained from this article and other publications are evaluated to prove the accuracy of the proposed theory and the calculation program. Then, a parameter study is carried out to capture the effect of some material and geometrical parameters on the static response of structures. Especially the influence of the flexoelectric effect and discontinuous foundation is investigated. As two elastic foundation parameters and flexoelectric coefficient are increased, the non-dimensional maximum deflection of the plate decreases, indicating that these factors improve the plate's stiffness.

**Keywords:** *Nanoplates; discontinuous elastic foundation; flexoelectricity; static bending; finite element method.*

## **1. Introduction**

Nanostructures are currently widely used in engineering as sensors, actuators, and energy harvesters. Flexoelectricity is common in these structures due to strain gradients. Several studies have revealed that nanoplate mechanical behavior involves a flexoelectric effect. Yan [1] used an analytical solution to study static bending and free vibration of piezoelectric nanoplates. To show the piezoelectric and flexoelectric effects of nanoplates, Yang et al. [2] devised an analytical solution. In this case, the authors applied the classical plate theory (CPT). The CPT equations were solved analytically, revealing the flexoelectric impact on the plate's mechanical response. The static bending response of flexoelectric nanoplates with one edge clamped was determined using finite difference. The precise solution and classical plate theory were used to examine the buckling response of flexoelectric nanoplates by Ebrahimi<sup>1</sup> and Barati [3]. Amin et al. [4] evaluated the nonlinear free vibration of functionally graded flexoelectric nanoplates

---

\* Email: minhphv@lqdtu.edu.vn

using classical plate theory and flexoelectric theory. Amir et al. [5] explored the free vibration of sandwich flexoelectric plates using Navier's approach. It was used to find the displacement and electric field of these plates subjected to the thermo-electro-magnetic force. They investigated the static bending behavior of FG nanoplates under thermal, electric, and flexoelectric fields. It is based on Kirchhoff's classical plate theory. Ghobadi and his colleagues [6] studied the static bending response of FG nanoplates, taking into consideration the influences of temperature, electric, and flexoelectric fields. Giannakopoulos et al. [7] developed an antiplane dynamic flexoelectric problem, which was described as a dielectric solid with electric polarization and flexoelectricity gradients due to strain gradients. Qu and colleagues [8] examined the torsion of a rectangular cross-section flexoelectric semiconductor rod. Yang et al. [9] explored multilayer photonic crystal band architectures with flexoelectricity. In this study, the traditional plate theory of Kirchhoff was employed to develop the finite element formulations. Readers can find more interesting works related to imperfect structures as well as the flexoelectric effect in these documents [10-16].

## 2. Finite element formulations of the nanoplate taking into consideration the flexoelectric effect

The rectangular plate is defined geometrically by its length  $a$ , breadth  $b$ , and thickness  $h$ . The plate is supported on a discontinuous elastic foundation with two coefficients  $k_w$  and  $k_s$  (Fig. 1).

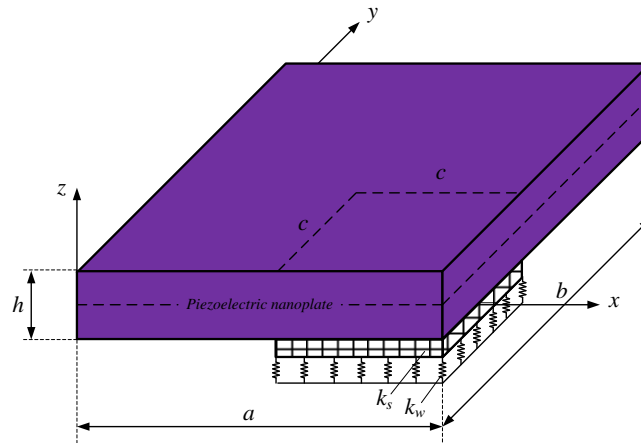


Fig. 1. The nanoplate partially resting on a discontinuous elastic foundation.

This work uses hyperbolic sine functions [17], the displacement field at any location on the plate is stated as follows:

$$u_x = -z \frac{\partial w_b}{\partial x} - f(z) \frac{\partial w_s}{\partial x}; v_y = -z \frac{\partial w_b}{\partial y} - f(z) \frac{\partial w_s}{\partial y}; w_z = w_b + w_s \quad (1)$$

in which  $f(z) = z - \zeta(z)$ ,  $\zeta(z) = h \sin \frac{z}{h} - z \cosh \frac{1}{2}$ ;  $u_x$ ,  $v_y$ , and  $w_z$  are the displacements in the  $x$ -,  $y$ -, and  $z$ -directions at one point within the plate;  $w_b$  and  $w_s$  are the bending displacement and shear displacement in the  $z$ -direction [17].

Herein, the essence of using the shear strain correction function  $f(z)$  is to increase the accuracy more than choosing a constant correction factor (as used by the classical theory), especially for plate and shell structures of medium and large thickness. But the requirement of the selection function is that the shear stress on the free surfaces of the plate (shell) is zero, which leads to  $1 - f'(z) = 0$  when  $z = \pm \frac{h}{2}$ .

Derivative of displacement one obtains deformation components with respect to coordinates.

$$\boldsymbol{\varepsilon} = \mathbf{z} \cdot \left\{ \varepsilon_{bx} \quad \varepsilon_{by} \quad \gamma_{bxy} \right\}^T + f(z) \left\{ \varepsilon_{sx} \quad \varepsilon_{sy} \quad \gamma_{sxy} \right\}^T; \boldsymbol{\gamma} = \frac{\partial \zeta(z)}{\partial z} \left\{ \gamma_{xz} \quad \gamma_{yz} \right\}^T \quad (2)$$

where  $\varepsilon_{bx} = \frac{\partial^2 w_b}{\partial x^2}$ ,  $\varepsilon_{by} = \frac{\partial^2 w_b}{\partial y^2}$ ,  $\gamma_{bxy} = \frac{\partial^2 w_b}{\partial x \partial y}$ ,  $\varepsilon_{sx} = \frac{\partial^2 w_s}{\partial x^2}$ ,  $\varepsilon_{sy} = \frac{\partial^2 w_s}{\partial y^2}$ ,  $\gamma_{sxy} = 2 \frac{\partial^2 w_s}{\partial x \partial y}$ ,  $\gamma_{xz} = \frac{\partial w_s}{\partial x}$ ,  $\gamma_{yz} = \frac{\partial w_s}{\partial y}$ .

This research makes the assumption that the strain gradient in the thickness direction is substantially less than the strain gradients in the  $x$ - and  $y$ -axes, and that the  $z$ -axis strain gradient is ignored. The strain gradient is composed of the following components [13, 14]:

$$\boldsymbol{\eta} = \boldsymbol{\eta}_b + \frac{\partial f(z)}{\partial z} \boldsymbol{\eta}_s \quad (3)$$

When the flexoelectric effect is taken into consideration, the stress components and electric displacement vector of a nanoscale dielectric material are as follows:

$$T_{ij} = c_{ijkl} \varepsilon_{kl} - e_{kij} E_k; \Psi_{ijm} = -f_{kijm} E_k; P_i = c_{ijk} \varepsilon_{jk} + \kappa_{ij} E_k + f_{ijkl} \eta_{jkl} \quad (4)$$

in which  $c_{ijkl}$ ,  $e_{kij}$ ,  $f_{kijm}$  and  $\kappa_{ij}$  are the components of elastic, piezoelectric, flexoelectric and permittivity constant tensor; they are the material parameters.  $T_{ij}$  is the stress tensor, which is similar to that of the traditional elastic foundation.  $P_i$  is the electric displacement vector, and  $\Psi_{ijm}$  is the moment stress tensor or the higher-order stress tensor [13, 14]. The following particular stress and electric displacement vector expressions:

$$\mathbf{T} = \mathbf{C}_b \boldsymbol{\varepsilon} - \tilde{\mathbf{E}}; \mathbf{S} = \mathbf{C}_s \boldsymbol{\gamma}; \boldsymbol{\Psi} = \begin{Bmatrix} \Psi_{xxz} \\ \Psi_{yyz} \end{Bmatrix} = -f_{14} \begin{Bmatrix} 1 \\ 1 \end{Bmatrix} E_z; P_z^0 = e_{31} (\varepsilon_{xx} + \varepsilon_{yy}) + \kappa_{33} E_z + f_{14} (\eta_{xxz} + \eta_{yyz}) \quad (5)$$

where  $f_{3113} = f_{3223} = f_{14}$  [18].

The electrical field is computed in the following manner from the partial derivative of the electrical potential:

$$E_z = -\frac{\partial \varphi}{\partial z}; \frac{\partial P_z^0}{\partial z} = 0 \quad (6)$$

From equations (5) and (6), one gets:

$$\varphi = \frac{e_{31}}{2a_{33}} \left( \frac{\partial^2 w}{\partial x^2} + \frac{\partial^2 w}{\partial y^2} \right) z^2 + c_1 + c_2 z \quad (7)$$

where  $c_1$  and  $c_2$  are the unknown coefficients. We have the following conditions under the open-circuit condition:

$$P_z^0 \left( \pm \frac{h}{2} \right) = 0; c_2 = -\frac{f_{14}}{a_{33}} \left( \frac{\partial^2 w}{\partial x^2} + \frac{\partial^2 w}{\partial y^2} \right) \quad (8)$$

By substituting equations (8) and (7) into equation (6), the internal electric field is expressed as follows:

$$E_z = \frac{e_{31}}{\kappa_{33}} \left( \frac{\partial^2 w_b}{\partial x^2} + \frac{\partial^2 w_b}{\partial y^2} \right) z + \frac{e_{31}}{\kappa_{33}} \left( \frac{\partial^2 w_s}{\partial x^2} + \frac{\partial^2 w_s}{\partial y^2} \right) f(z) + \frac{f_{14}}{\kappa_{33}} \left( \frac{\partial^2 w_b}{\partial x^2} + \frac{\partial^2 w_b}{\partial y^2} \right) + \frac{f_{14}}{\kappa_{33}} \left( \frac{\partial^2 w_s}{\partial x^2} + \frac{\partial^2 w_s}{\partial y^2} \right) \frac{\partial f(z)}{\partial z} \quad (9)$$

The electric Gibbs free energy in an open circuit has the following form:

$$\Pi = \frac{1}{2} \int_V (\boldsymbol{\varepsilon}^T \mathbf{T} + \boldsymbol{\gamma}^T \mathbf{S} + \boldsymbol{\eta}^T \boldsymbol{\Psi}) dV \quad (10)$$

where  $k_w$  and  $k_s$  are the two coefficients of the Pasternak elastic foundation. Thus, for the nanoplates, taking into account the variable composition of the strain as equation (3). This results in the plate energy expression with the final addition as in equation (10). This is completely different from the ordinary plate. The nanoplate is divided into 4 node elements, each node has 6 degrees of freedom:

$$\boldsymbol{\psi}_e = \sum_{i=1}^4 \left\{ w_{bi}, w_{si}, \left( \frac{\partial w_b}{\partial x} \right)_i, \left( \frac{\partial w_s}{\partial x} \right)_i, \left( \frac{\partial w_b}{\partial y} \right)_i, \left( \frac{\partial w_s}{\partial y} \right)_i \right\}^T; w_b = \mathbf{H}_b \boldsymbol{\psi}_e; w_s = \mathbf{H}_s \boldsymbol{\psi}_e \quad (11)$$

where  $H_j$  is the Hermit interpolation functions.

The displacement vector at any position inside the element is then interpolated via the nodal displacement vector of the element, and strain vectors are calculated as follows using the nodal displacement vector:

$$\mathbf{u} = \mathbf{H} \cdot \boldsymbol{\psi}_e; \boldsymbol{\varepsilon}_b = \mathbf{B}_1 \boldsymbol{\psi}_e; \boldsymbol{\varepsilon}_s = \mathbf{B}_2 \boldsymbol{\psi}_e; \gamma_0 = \mathbf{B}_3 \boldsymbol{\psi}_e; \boldsymbol{\eta}_b = \mathbf{B}_4 \boldsymbol{\psi}_e; \boldsymbol{\eta}_s = \mathbf{B}_5 \boldsymbol{\psi}_e \quad (12)$$

Equation (10) and the external force exerted on the plate may be expressed succinctly as follows:

$$\Pi_e = (1/2) \boldsymbol{\psi}_e^T \mathbf{K}_e \boldsymbol{\psi}_e; W_e = \boldsymbol{\psi}_e^T \mathbf{P}_e \quad (13)$$

Using the principle of minimal energy (which includes deformation potential and external force work)  $\delta \Pi_e = \delta W_e$ , then assembling the matrix and removing the boundary condition, the derived plate's static equilibrium equation has the following form:

$$\mathbf{K} \mathbf{q} = \mathbf{F} \quad (14)$$

### 3. Verification study

**Example 1:** A simply supported (SSSS) nanoplate with the following parameters:  $h = 20$  nm,  $a = b = 50h$ , and material properties  $c_{11} = 102$  GPa;  $c_{12} = 31$  GPa;  $c_{33} = 35.50$  GPa;  $e_{31} = -17.05$  C/m<sup>2</sup>;  $k_{33} = 1.76 \cdot 10^{-8}$  C/(Vm);  $f_{14} = 10^{-7}$  C/m is considered. The plate is forced evenly with  $q_0 = 0.05$  MPa. Figure 4 compares the numerical findings of our study to those of Yang et al.'s analytical solution [2].

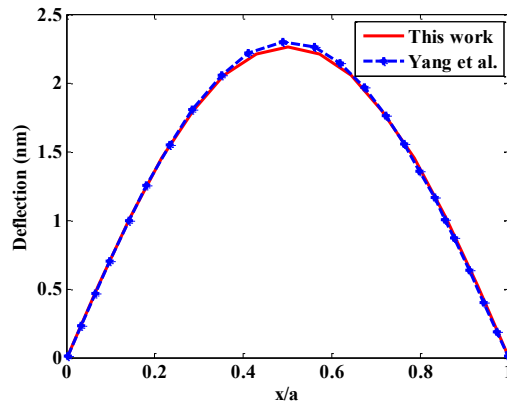


Fig. 2. Non-dimensional deflection at  $y = b/2$  taking into account the flexoelectric effect.

**Example 2:** Consider a plate with the dimensions  $a = b = 0.2$  m,  $h = a/10$ , and  $a/200$  lying on an elastic basis.  $E = 320.24$  GPa, and Poisson's ratio of 0.26 are the material characteristics. The plate is SSSS and is loaded evenly  $q_0$ . Non-dimensional elastic foundation and deflection at the plate's center point are determined as follows:

$$K_w^* = \frac{K_w a^4}{D}; K_s^* = \frac{K_s a^2}{D}; \bar{w} = \frac{10^3 D}{q_0 a^4} w\left(\frac{a}{2}, \frac{b}{2}\right); D = \frac{Eh^3}{12(1-\nu^2)} \quad (15)$$

Table 1 compares the accuracy of our work, the differential quadrature approach [19], and the analytical method [20] with increasing mesh size.

*Table 1. Non-dimensional deflection  $\bar{w}$  of the plate resting on the two-parameter elastic foundation*

$K_w^*$	$K_s^*$	$a/h = 10$					
		[19]	[20]	This work			
				8x8 elements	10x10 elements	12x12 elements	14x14 elements
1	5	3.3455	3.3455	3.3797	3.3643	3.3560	3.3512
	10	2.7505	2.7504	2.7743	2.7635	2.7578	2.7545
	15	2.3331	2.3331	2.3508	2.3428	2.3386	2.3361
	20	2.0244	2.0244	2.0382	2.0320	2.0287	2.0268
81	5	2.8422	2.8421	2.8667	2.8557	2.8499	2.8464
	10	2.3983	2.3983	2.4163	2.4083	2.4040	2.4015
	15	2.0730	2.0730	2.0868	2.0806	2.0774	2.0755
	20	1.8245	1.8244	1.8355	1.8306	1.8280	1.8265
625	5	1.3785	1.3785	1.3835	1.3816	1.3804	1.3797
	10	1.2615	1.2615	1.2658	1.2642	1.2632	1.2626
	15	1.1627	1.1627	1.1665	1.1650	1.1642	1.1637
	20	1.0782	1.0782	1.0815	1.0802	1.0795	1.0791

#### 4. Numerical results

In this section, two types of boundary conditions are taken into the calculation: SSSS and cantilever (CFFF) plates. Consider an SSSS nanoplate with  $h = 20$  nm,  $a = b = 50h$ , and the material properties are  $c_{11} = 102$  GPa;  $c_{12} = 31$  GPa;  $c_{33} = 35.50$  GPa;  $e_{31} = -17.05$  C/m<sup>2</sup>;  $k_{33} = 1.76 \cdot 10^{-8}$  C/(Vm). The plate is rested on a discontinuous two-parameter elastic foundation with  $k_w$  and  $k_s$ . A uniformly distributed load is uniformly applied to a plate of magnitude  $P_0$ . Two elastic foundation parameters are  $k_1^* = 100$ ,  $k_2^* = 10$ , where non-dimensional parameters are calculated as follows:

$$w^* = \frac{10^3 c_{11} h_0^3}{12 P_0 a^4} w; f_{14}^* = \frac{f_{14}}{f_{14}^0}; k_1^* = \frac{k_w a^4}{D_f}; k_2^* = \frac{k_s a^2}{D_f}; D_f = \frac{c_{11} h_0^3}{12}; f_{14}^0 = 10^{-7} C/m; h_0 = a/50 \quad (16)$$

#### 4.1. Influence of the discontinuous elastic foundation

Change the elastic foundation's length  $c$  such that the  $c/a$  ratio ranges between 0 and 1/2. The displacement response  $w^*$  of the nanoplate along the  $y = b/2$  direction is presented in Fig. 3. The results of the calculations indicate that as the elastic foundation area increases, the plate gets stronger and its maximum displacement lowers. When a plate is supported by an SSSS boundary (symmetrical form), the plate's displacement route is no longer symmetrical through the location  $x = a/2$ , and the position of the maximum displacement tends to move to the right.

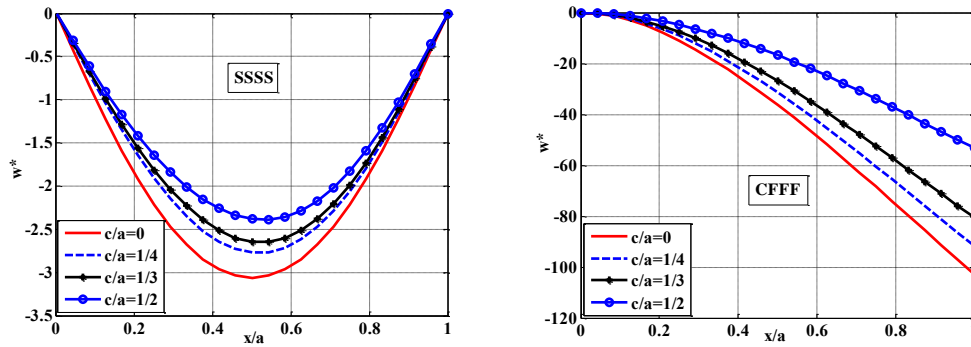


Fig. 3. The variation of displacement  $w^*(y = b/2)$  depends on the length  $c$  of the elastic foundation.

#### 4.2. Influence of the flexoelectric effect

To show the effect of parameter  $f_{14}$ , the coefficient  $f_{14}^*$  is varied between 0 and 4, with 0 corresponding to the scenario of disregarding the flexoelectric effect.

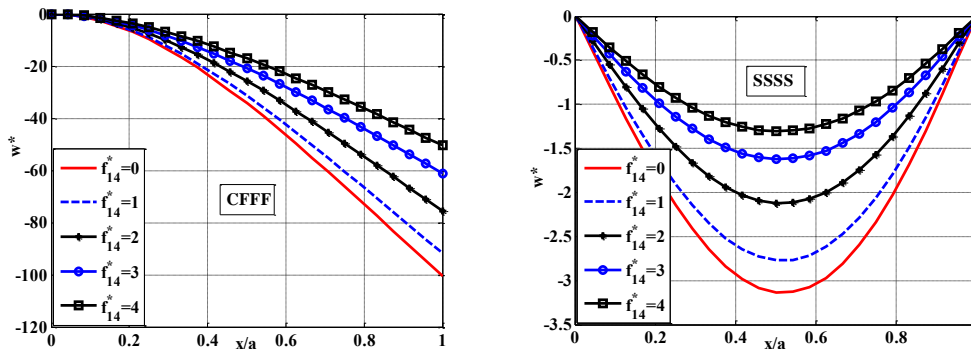


Fig. 4. The displacement change  $w^*(y = b/2)$  is dependent on  $f_{14}$ ,  $c/a = 1/4$ .

The displacement response between the panels  $w^*(y = b/2)$  is calculated as illustrated in Fig. 4. When the flexoelectric effect is included (i.e.  $f_{14}$  is greater than zero), the plate's maximum displacement is lowered. For the SSSS plate, as the coefficient  $f_{14}$  grows, the plate's deflection line  $w^*$  becomes less deflected relative to  $x = a/2$ .

#### 4.3. Effect of plate thickness $h$

By varying the plate thickness  $h$ , the ratio  $a/h$  may be varied between 50 and 100. The results of the plate's static bending reaction are displayed in Fig. 5. As the plate thickness lowers, the plate's maximum displacement rises. For a plate exposed to the SSSS boundary, the thinner the plate thickness is, the stronger the impact of the elastic foundation is, and the farther to the left the displacement line  $w^*(b/2)$  deviates from the  $x = a/2$  position.

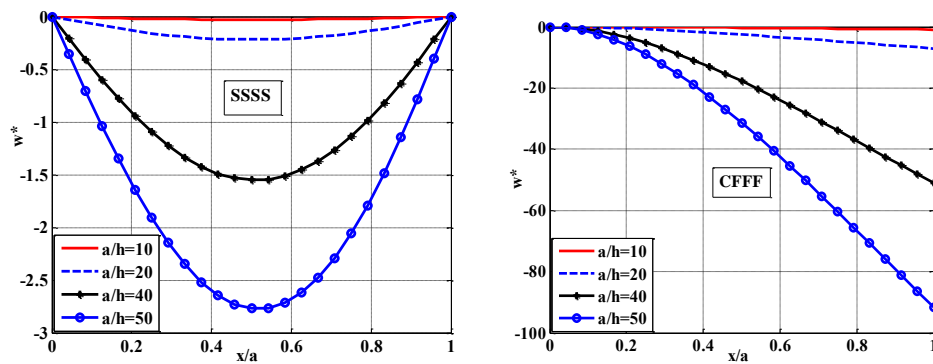


Fig. 5. The displacement change  $w^*(y = b/2)$  is dependent on the plate thickness  $h$ .

## 5. Conclusions

The static bending response of nanoplates, including the flexoelectric effect, is explored in this research utilizing the novel shear strain theory in combination with the finite element method. The plate is partially supported by a two-factor elastic foundation. This research comes to the following key findings. As the coefficient  $f_{14}$  is increased, the maximum displacement  $w^*$  of the plate decreases, indicating that the coefficient  $f_{14}$  improves the plate's stiffness. As the thickness of the plate decreases, the plate's displacement rises. The influence of the discontinuous elastic foundation is also very obvious. As the elastic foundation area increases, the maximum displacement of the plate decreases, whereas the maximum displacement of the plate for the SSSS boundary is shifted to the right at  $x = a/2$ .



## References

- [1] Z. Yan, "Size-dependent bending and vibration behaviors of piezoelectric circular nanoplates," *Smart Mater. Struct.*, vol. 25, no. 3, 2016, DOI: 10.1088/0964-1726/25/3/035017
- [2] W. Yang, X. Liang, and S. Shen, "Electromechanical responses of piezoelectric nanoplates with flexoelectricity," *Acta Mech.*, vol. 226, no. 9, pp. 3097-3110, 2015, DOI: 10.1007/s00707-015-1373-8
- [3] F. Ebrahimi and M. R. Barati, "Static stability analysis of embedded flexoelectric nanoplates considering surface effects," *Appl. Phys. A Mater. Sci. Process.*, vol. 123, no. 10, 2017, DOI: 10.1007/s00339-017-1265-y
- [4] A. Ghobadi, Y. T. Beni, and H. Golestanian, "Nonlinear thermo-electromechanical vibration analysis of size-dependent functionally graded flexoelectric nano-plate exposed magnetic field," *Arch. Appl. Mech.*, vol. 90, no. 9, pp. 2025-2070, 2020, DOI: 10.1007/s00419-020-01708-0
- [5] S. Amir, H. BabaAkbar-Zarei, and M. Khorasani, "Flexoelectric vibration analysis of nanocomposite sandwich plates," *Mech. Based Des. Struct. Mach.*, vol. 48, no. 2, pp. 146-163, 2020, DOI: 10.1080/15397734.2019.1624175
- [6] A. Ghobadi, Y. T. Beni, and H. Golestanian, "Size dependent thermo-electro-mechanical nonlinear bending analysis of flexoelectric nano-plate in the presence of magnetic field," *Int. J. Mech. Sci.*, vol. 152, pp. 118-137, 2019, DOI: 10.1016/j.ijmecsci.2018.12.049
- [7] A. E. Giannakopoulos and T. Zisis, "Steady-state antiplane crack considering the flexoelectrics effect: surface waves and flexoelectric metamaterials," *Arch. Appl. Mech.*, vol. 91, no. 2, pp. 713-738, 2021, DOI: 10.1007/s00419-020-01815-y
- [8] Y. Qu, F. Jin, and J. Yang, "Torsion of a flexoelectric semiconductor rod with a rectangular cross section," *Arch. Appl. Mech.*, vol. 91, no. 5, pp. 2027-2038, 2021, DOI: 10.1007/s00419-020-01867-0
- [9] W. Yang, T. Hu, X. Liang, and S. Shen, "On band structures of layered phononic crystals with flexoelectricity," *Arch. Appl. Mech.*, vol. 88, no. 5, pp. 629-644, 2018, DOI: 10.1007/s00419-017-1332-z
- [10] D. D. Nguyen, Q. Q. Tran, and D. K. Nguyen, "New approach to investigate nonlinear dynamic response and vibration of imperfect functionally graded carbon nanotube reinforced composite double curved shallow shells subjected to blast load and

- temperature,” *Aerosp. Sci. Technol.*, vol. 71, pp. 360-372, 2017, DOI: 10.1016/j.ast.2017.09.031
- [11] N. D. Duc, “Nonlinear static and dynamic stability of functionally graded plates and shells,” *Vietnam Vietnam Natl Univ Press*, p. 724, 2014.
- [12] N. D. Duc and T. Q. Quan, “Nonlinear response of imperfect eccentrically stiffened FGM cylindrical panels on elastic foundation subjected to mechanical loads,” *Eur. J. Mech. A/Solids*, vol. 46, pp. 60-71, 2014, DOI: 10.1016/j.euromechsol.2014.02.005
- [13] D. H. Duc, D. Van Thom, P. H. Cong, P. Van Minh, and N. X. Nguyen, “Vibration and static buckling behavior of variable thickness flexoelectric nanoplates,” *Mech. Based Des. Struct. Mach.*, 2022, DOI: 10.1080/15397734.2022.2088558
- [14] L. M. Thai, D. T. Luat, V. B. Phung, P. Van Minh, and D. Van Thom, “Finite element modeling of mechanical behaviors of piezoelectric nanoplates with flexoelectric effects,” *Arch. Appl. Mech.*, vol. 92, no. 1, pp. 163-182, 2022, DOI: 10.1007/s00419-021-02048-3
- [15] N. C. Tho, N. T. Thanh, T. D. Tho, P. Van Minh, and L. K. Hoa, “Modelling of the flexoelectric effect on rotating nanobeams with geometrical imperfection,” *J. Brazilian Soc. Mech. Sci. Eng.*, vol. 43, no. 11, 2021, DOI: 10.1007/s40430-021-03189-w
- [16] D. Van Thom, D. H. Duc, P. Van Minh, and N. S. Tung, “Finite Element Modelling for Free Vibration Response of Cracked Stiffened Fgm Plates,” *Vietnam J. Sci. Technol.*, vol. 58, no. 1, p. 119, 2020, DOI: 10.15625/2525-2518/58/1/14278
- [17] H. T. Thai and D. H. Choi, “Finite element formulation of various four unknown shear deformation theories for functionally graded plates,” *Finite Elem. Anal. Des.*, vol. 75, pp. 50-61, 2013, DOI: 10.1016/j.finel.2013.07.003
- [18] L. Shu, X. Wei, T. Pang, X. Yao, and C. Wang, “Symmetry of flexoelectric coefficients in crystalline medium,” *J. Appl. Phys.*, vol. 110, no. 10, 2011, DOI: 10.1063/1.3662196
- [19] J. B. Han and K. M. Liew, “Numerical differential quadrature method for Reissner/Mindlin plates on two-parameter foundations,” *Int. J. Mech. Sci.*, vol. 39, no. 9, pp. 977-989, 1997, DOI: 10.1016/s0020-7403(97)00001-5
- [20] H. T. Thai, M. Park, and D. H. Choi, “A simple refined theory for bending, buckling, and vibration of thick plates resting on elastic foundation,” *Int. J. Mech. Sci.*, vol. 73, pp. 40-52, 2013, DOI: 10.1016/j.ijmecsci.2013.03.017

## PHÂN TÍCH UỐN TĨNH CỦA TẤM NANO TRÊN NỀN ĐÀN HỒI KHÔNG LIÊN TỤC KỂ ĐẾN HIỆU ỨNG FLEXOELECTRICITY

**Phùng Văn Minh, Lê Minh Thái, Đoàn Trắc Luật, Nguyễn Đình Anh Vũ**

**Tóm tắt:** Trong nghiên cứu này, các tấm hình chữ nhật chịu tải trọng tĩnh và được hỗ trợ trên nền đàn hồi hai tham số không liên tục được phân tích. Các công thức tính toán được phát triển từ lý thuyết biến dạng cắt cải tiến, trong đó chuyển vị  $w$  được chia thành các thành phần biến dạng uốn và biến dạng cắt. Các kết quả thu được từ bài báo này và các công trình khác được đánh giá để chứng minh tính chính xác của lý thuyết đề xuất và chương trình tính toán. Sau đó, một nghiên cứu tham số được thực hiện để xem xét ảnh hưởng của một số thông số về vật liệu và hình học đến đáp ứng tĩnh của kết cấu. Đặc biệt là ảnh hưởng của hiệu ứng uốn điện và nền không liên tục được khảo sát. Khi hai thông số của nền đàn hồi và hệ số flexoelectric tăng lên thì chuyển vị không thứ nguyên lớn nhất của tấm giảm đi. Điều này cho thấy các yếu tố này cải thiện độ cứng của kết cấu.

**Từ khóa:** Tấm nano; nền đàn hồi không liên tục; hiệu ứng flexoelectricity; uốn tĩnh; phân tử hữu hạn.

Received: 25/05/2022; Revised: 11/10/2022; Accepted for publication: 11/11/2022

